A Study of the Magnus Effects on a Sounding Rocket at Supersonic Speeds

JAMES C. USELTON* AND JACK B. CARMAN†
ARO Inc., Arnold Air Force Station, Tenn.

A study of the Magnus effects was made for a 0.355-scale model of the Apache sounding rocket at Mach numbers 2–6. Freestream Reynolds number, based on model length, was varied between 1.8×10^6 and 23.9×10^6, and angle of attack varied from $-5°$ to $15°$. The model was tested without fins at spin rates up to 4000 rpm and with fins at cant angles of 0, $-1°$, and $\pm 2°$, which produced spin rates ranging from about -3200 to 3200 rpm. Tests of the complete spinning model showed significant changes in the Magnus forces and moments with angle of attack, Mach number, and Reynolds number. Tests of the spinning model with and without fins and static tests with different fin combinations allowed a degree of assessment of the different type Magnus effects.

Nomenclature

A	=	reference area, model base area, 4.191 in.^{2}
C_m	=	pitching-moment coefficient, pitching moment/$q_\infty Ad$
C_N	=	normal-force coefficient, normal force/$q_\infty A$
C_n	=	yawing-moment coefficient, yawing moment/$q_\infty Ad$ (see Fig. 1)
C_{n_p}	=	yawing-moment coefficient derivative, $\partial C_n/\partial(pd/2V_\infty)$
C_Y	=	side-force coefficient, side force/$q_\infty A$ (see Fig. 1)
C_{Y_p}	=	side-force coefficient derivative, $\partial C_Y/\partial(pd/2V_\infty)$
d	=	model base diameter, 2.310 in.
l	=	model length, 49.766 in.
M_∞	=	freestream Mach number
p	=	model spin rate (positive, clockwise viewing from base), rpm or rad/sec
$pd/2V_\infty$	=	spin parameter or helix angle, rad
q_∞	=	freestream dynamic pressure, psia
Re_l	=	freestream Reynolds number based on model length
V_∞	=	freestream velocity, fps
x	=	fin span distance, in.
α	=	angle of attack, deg
δ	=	fin cant angle (positive angles produce positive spin rates), deg
ϕ	=	model roll angle, deg

Introduction

SOUNDING rockets of high fineness ratio are susceptible to large angular motions when perturbations are introduced at burnout. Six-degree-of-freedom stability analysis of these vehicles requires knowledge of the Magnus characteristics. Therefore, this program was initiated to make a thorough study of the Magnus effects on a model of the Apache sounding rocket.

The Nike-Apache or Nike-Cajun is a two-stage solid-propellant rocket vehicle, jointly developed by NASA and the University of Michigan as a meteorological sounding rocket system. These rocket systems have been successfully used in flight investigations to measure atmospheric densities and winds, and to photograph hurricanes. These missions were successful as long as the vehicle had a reasonable static margin and flew zero lift and nonspinning trajectories. Some systems were spun up during flight either to satisfy payload requirements or for range safety reasons, and some of these flights resulted in the Apache vehicle experiencing angular motions which were unexpectedly large. For example, some vehicles went dynamically unstable and coned through large angles; others had their flights terminated abruptly because of structural failure. As a result of these flights, the roll characteristics of the Apache were investigated and are reported in Ref. 1.

In the present wind-tunnel test program, force data were obtained on a 0.355-scale Apache model (Fig. 1) at Mach numbers 2, 3, 4, 5, and 6, and at Reynolds numbers (Re_l) ranging from 1.8 million to 23.9 million. The angle of attack (α) range was from $-5°$ to $15°$. The model was tested with and without fins, and the spin rate varied between 0 and ~4000 rpm.

Apparatus and Procedure

Tunnel A is a continuous, closed-circuit, variable-density wind tunnel with an automatically driven flexible-plate-type nozzle (the nozzle is flexible in the model β plane) and a 40- × 40-in. test section. It can be operated at Mach numbers from 1.5 to 6 at maximum stagnation pressures from 29 to 200 psia, respectively, and stagnation temperatures up to 750°F ($M_\infty = 6$). Minimum operating pressures range

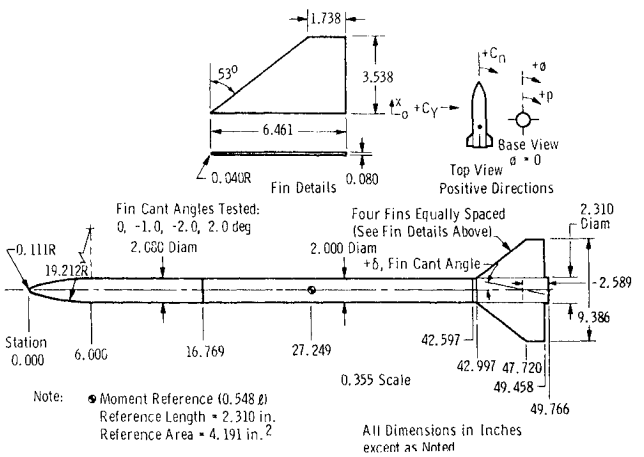

Fig. 1 Details of 0.355-scale Apache model.

Presented as Paper 70-207 at the AIAA 8th Aerospace Sciences Meeting, New York, January 19–21, 1970; submitted February 19, 1970; revision received November 12, 1970. This work was sponsored by the Air Force Armament Laboratory (AFATL), Air Force Systems Command (AFSC) at the Arnold Engineering Development Center (AEDC), under Contract F40600-69-C-0001 with ARO Inc.

* Project Engineer, Supersonic-Hypersonic Branch, Aerodynamics Division, von Karman Facility (VKF). Member AIAA.

† Project Engineer, Supersonic-Hypersonic Branch, Aerodynamics Division, von Karman Facility.

from about $\frac{1}{10}$ to $\frac{1}{20}$ of the maximum at each Mach number.

The model (Fig. 1) is essentially an ogive cylinder with cruciform 53° swept fins mounted at the model base, and it has a fineness ratio of 24.88. It was mounted on two ball bearings with their inner races fixed to an inner shell that was attached to the balance forward taper. The model spin rates with the fins on were obtained by canting the fins at angles of 0, $-1°$ and $\pm 2°$ with an accuracy on the fin cant angle of ± 3 min. For the no-fin configuration, spin rates were obtained by directing jets of nitrogen on the model base, which was machined with small slanted cups for spinning. All model configurations were dynamically balanced.

The VKF four-component balance was used for the tests. The small outrigger side beams of the balance, with semiconductor strain gages, were used to obtain the sensitivity required to measure small side loads accurately while maintaining adequate balance stiffness for the larger pitch loads. When a yawing moment is imposed on the balance, secondary bending moments are induced in the side beams. Thus, the outrigger beams act as mechanical amplifiers, and a normal-force to side-force capacity ratio of 20 was achieved by a 500-lb normal force loading. Before the tests, a range of static loads was applied to the balance to simulate the model loads anticipated during testing. All balance components were loaded simultaneously, and a range of uncertainties in measurement was determined from the differences between the applied loadings and the values calculated by the balance calibration equations used in the final data reduction (Table 1).

For the zero spin data, the model was locked ($\phi = 0$) by pinning the outside shell of the model to the fixed inner shell. When the model was tested with the canted fins, it was allowed to spin freely at its steady-state value. Up to five data points were taken at each α when the model was spinning, whereas two or three data points were usually taken with the model locked (zero spin). The numerous data points were taken to average the scatter encountered because of model vibration and the small magnitude of the side forces.

For the no-fin spin data, the model was prespun to ~4000 rpm, and then data were recorded as the model spin rate decayed. Model spin rates were monitored using a photo cell-diode tachometer mounted inside the model.

The α was set within $\pm 0.01°$, and the model alignment with the wind-tunnel centerline in the β plane was within 1 min.

Results and Discussion

Background and Zero Spin Data

In 1966, a wind-tunnel program investigating the Magnus effects on the Tomahawk vehicle was conducted. The Tomahawk is a 23.3-fineness ratio sounding rocket with cruciform fins and is very similar to the Apache vehicle of this investigation. In the Tomahawk program, it was determined that as the angle of attack was increased, the leeward wake became characterized by a steady asymmetric vortex shape that produced side forces and moments on the model for the no-spin conditions. Also, it was found that the asymmetric leeward wake could cause the side force and moment curves for opposite directions of spin not to be mirror images with variation in α. Since the Apache model of the current test is so similar to the Tomahawk, similar trends in the data were expected. In the Tomahawk tests, the asymmetric wake effects were thoroughly investigated, and the complete results are presented in Refs. 2–4 along with the findings of other investigators pertaining to asymmetric leeward wake effects. Some of the asymmetric wake phenomenon follow.

Table 1 Loads and uncertainties for force balance

Balance component	Range of static loadings	Range of uncertainties
Normal force, lb	25–200	0.7–0.7
Pitching moment, in.-lb	250–1000	4.0–4.0
Side force, lb	1–6	0.015–0.015
Yawing moment, in.-lb	3–24	0.035–0.100

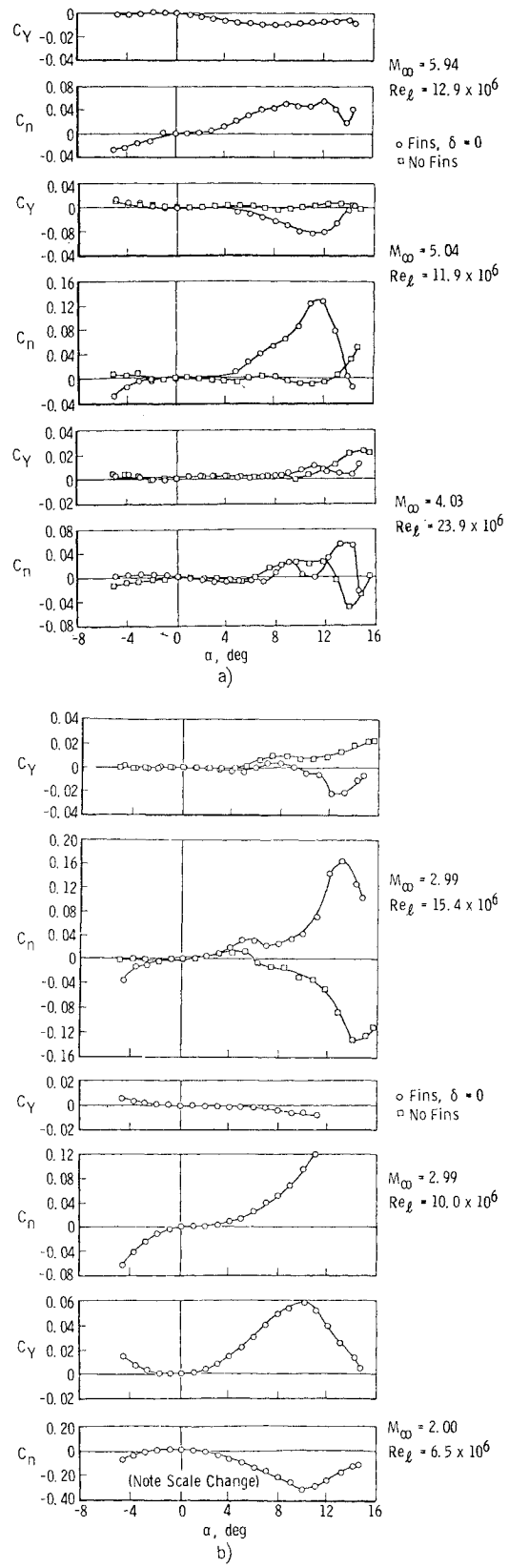

Fig. 2 Variations of C_Y and C_n with α for $p = 0$, fins-on ($\delta = 0$) and fins-off; a) $M_\infty = 2$ and 3, b) $M_\infty = 4$, 5, and 6.

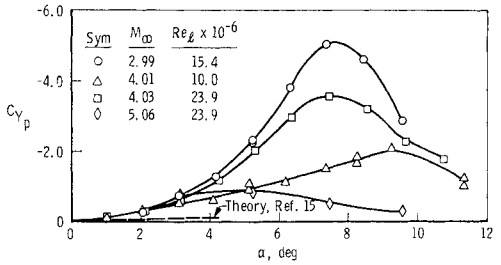

Fig. 3 Variations of C_{Y_p} with α for the fins-off configuration.

1) As α is increased on a missile-type body, the leeward wake changes from a steady symmetric pair of vortices to a steady asymmetric pattern of vortices and then to a system of unsteady vortices at the higher angles.[5,6] 2) Increasing the fineness ratio of a vehicle lowers the α at which the vortices become asymmetric.[7] 3) As α is increased on a high-fineness-ratio body, the vortices are shed along the body and new vortices form at the base.[8] 4) The direction that the vortices shift to become asymmetric should be arbitrary; however, many investigators[2,7,9,10] have found the pattern to be repeatable for a particular test set-up. It is possible that tunnel flow imperfections, model machining tolerances, etc., make the vortices prefer a particular direction. 5) The asymmetric vortex patterns produce side loads that oscillated with α on a nonspinning symmetrical model.[7,10]

As discussed previously, up to five data points were taken at each α to minimize extraneous points. All of the data points were plotted, and a weighted fairing was made through the data. The weighted data are presented in this report.

In Fig. 2 the variations in the side-force coefficient C_Y and yawing-moment coefficient C_n with α for the zero-spin conditions, fins on at zero cant angle ($\delta = 0, M_\infty = 2$–6) and fins off ($M_\infty = 3$, 4, and 5) are presented for various Reynolds numbers. The data indicate that an asymmetric vortex pattern was present and that the magnitude of its effect was reduced at the higher Mach numbers and Reynolds numbers. (The results for $M_\infty = 4.01$, $Re_l = 10.0 \times 10^6$, which are not shown, were very similar to those shown for $M_\infty = 2.99$, $Re_l = 15.4 \times 10^6$. Results for $M_\infty = 5.05$, $Re_l = 23.9 \times 10^6$ were rather similar to those for $M_\infty = 4.03$, $Re_l = 23.9 \times 10^6$.) The reduction with increasing Mach number was also noted by Gowen[7] and by Uselton.[2]

Magnus Effects on Canted Fin Vehicles

Spinning canted fin models are normally subject to Magnus effects primarily caused by the body, blanketing of the leeside fin, a fin base pressure Magnus effect, and the couple created by the axial components of the normal forces on the fins.[2,11–13] In addition to these more publicized Magnus effects, there may arise a Magnus force and moment from a body vortex interaction with the leeward fins. Since the leeward wake is asymmetric from the spin, the leeward fin could experience a side load from the vortex system.

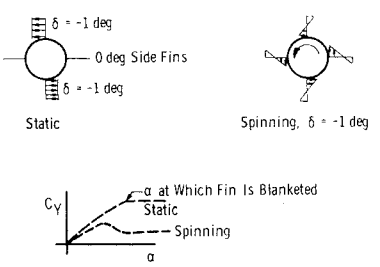

Fig. 4 Examination of the fin blanket magnus effect; illustrated fin pressure distribution at $\alpha = 0°$ and expected data trends.

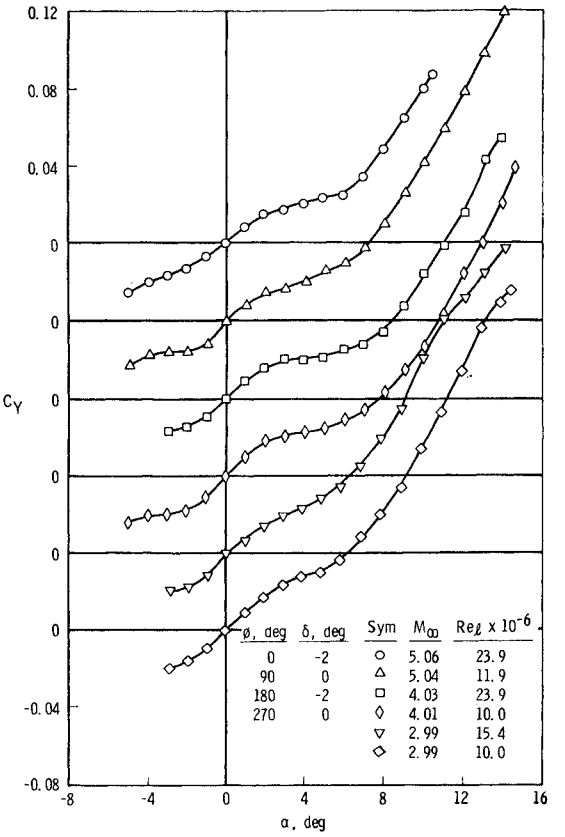

Fig. 5 Variations of C_Y with α, δ (side fins) = 0° and δ (leeward and windward) = −2°, $p = 0$.

An attempt was made to isolate the different types of Magnus forces and moments and to study them separately. The body Magnus effects are, of course, given by the fins-off configuration data. The variation of C_{Y_p} with α is presented for the fins-off configuration in Fig. 3. The coefficient decreases as M_∞ is increased from 3 to 5. C_{Y_p} and C_{n_p} (not shown) first increase with α and then tend toward zero at the higher angles. To understand this phenomenon, one must consider the zero spin data which show side forces and moments at the higher angles caused by the asymmetry of the leeside flow pattern. At the higher α's, the leeward wake becomes asymmetric for vehicles of this type (high-fineness ratio) regardless of spin rate. Therefore, at these higher α's the spin will influence the direction of the leeside wake asymmetry but not greatly affect the amount. The data also show larger Magnus effects at the higher Reynolds number at $M_\infty = 4$. This is unusual in that low-fineness-ratio vehicles normally have larger Magnus effects at lower Reynolds numbers.

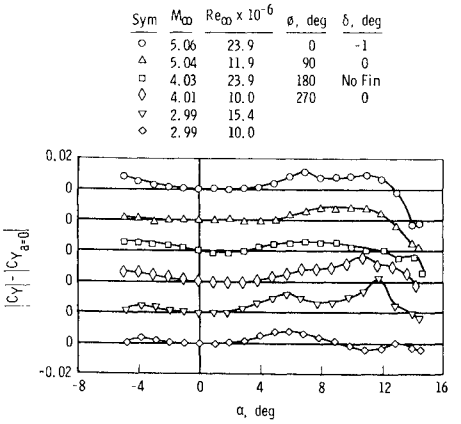

Fig. 6 Effects of blanketing the leeward fin, $p = 0$.

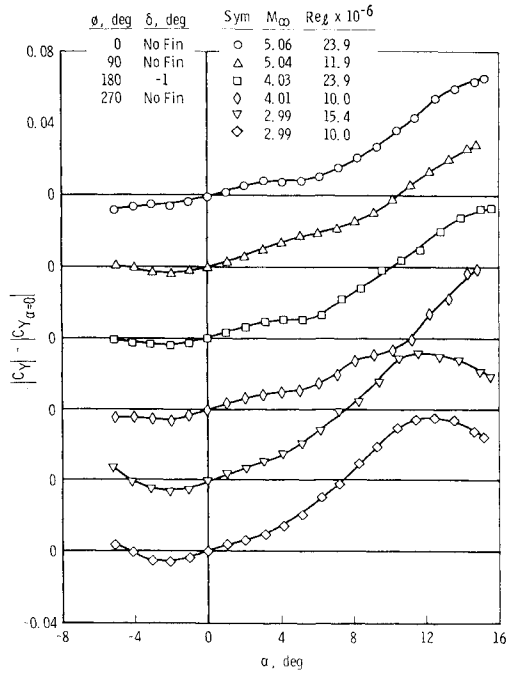

Fig. 7 Windward fin effects, $p = 0$.

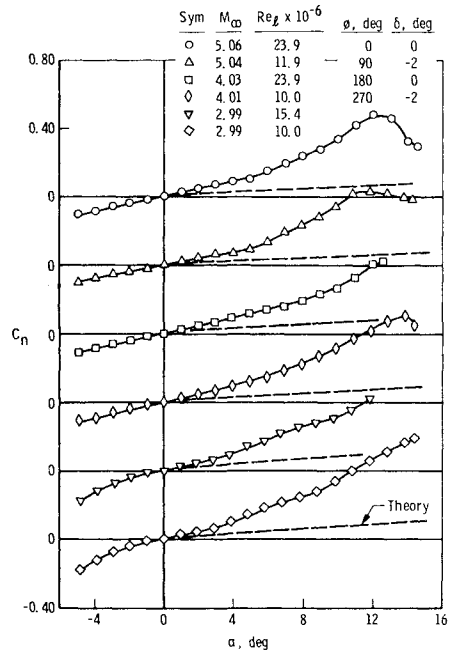

Fig. 9 Fin couple magnus effect, $p = 0$.

There is no applicable theory for analytically predicting the body Magnus force and moment for these test conditions. The only theory available considers only the shifting of the boundary layer and applies only to laminar incompressible boundary layers. The theory[14] shown with the data in Fig. 3, is much lower than the data but does predict the correct directions of the force and moment coefficient.

The fin blanket Magnus effect was investigated statically by testing with 0° fins on the sides and the −2° canted fins on top and bottom. Of course, the pressure distribution on the fins differ greatly between the static and spinning conditions as indicated in Fig. 4a. However, the static data would show where the fin became entirely blanketed (see Fig. 4b) and would give magnitudes that were known to be larger than the actual spinning case.

The static data with 0° fins on the sides and the −2° canted fins on the top and bottom are presented in Fig. 5 for $M_\infty = 3$, 4, and 5. The data show the correct signs but do not level off, indicating that the fin had become entirely blanketed. It was decided that possibly the windward fin could be contributing to the force since it would be moving into a higher energy flowfield as α was increased. Therefore, the model was tested with a −1° fin on top and 0° fins on the side. The windward or bottom fin was left off. The data presented as $|C_Y| - |C_{Y\alpha=0}|$ in Fig. 6 for $M_\infty = 3$, 4, and 5 should increase with α if there was a fin blanket effect, but they do not. The curves are near horizontal until, at the higher angles, the asymmetric vortex system apparently begins to act on the fins.

Since these data indicated that the blanketing of the top fin was small, it became apparent that the windward fin was contributing significantly to the net side force. Therefore, the model was tested statically with the −1° fin on the windward side only. These data are presented in Fig. 7 and show that the windward fin definitely contributed a substantial side force that increased continuously with α.

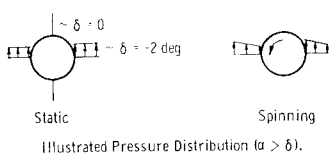

Fig. 8 Examination of the fin couple effect; illustrated pressure distribution ($\alpha > \delta$).

The model was statically tested with the −2° fins on the side and the 0° fins on the top and bottom to investigate yaw couple effect from the axial component of the fin normal force. The static pressure distribution on the side fins will differ from the spinning pressure distribution as illustrated in Fig. 8. The difference is smaller in this case, however, and the data should be of the same order of magnitude. An estimate of this couple calculated with freestream conditions approaching the fin is presented in Fig. 9, with the test data at $M_\infty = 3$, 4, and 5. The data show a much larger moment than that estimated, thus indicating that a more sophisticated analytical treatment of the flowfield approaching the fin would have to be used to obtain better estimates.

During earlier static tests[2] on a Tomahawk model, the leeward vortex shape was purposely made asymmetric with a grit strip down one side. This produced large side loads. Therefore, indications are that the body vortex system interacting on the fins can cause sizable Magnus effects. This may be more notable at the lower Mach numbers where the

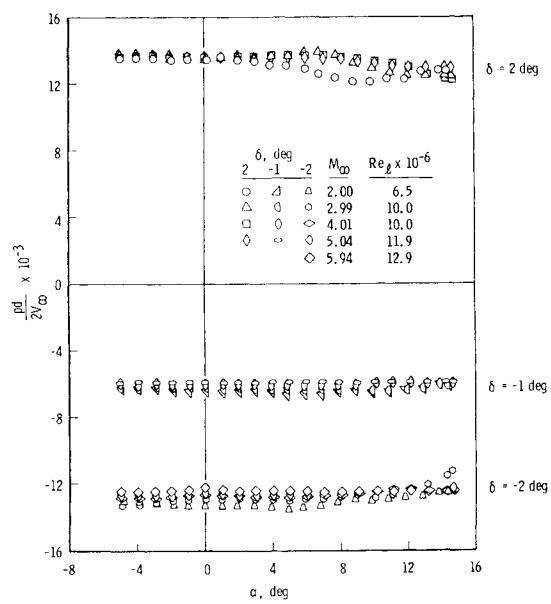

Fig. 10 Variation of spin parameter ($pd/2V_\infty$) with α.

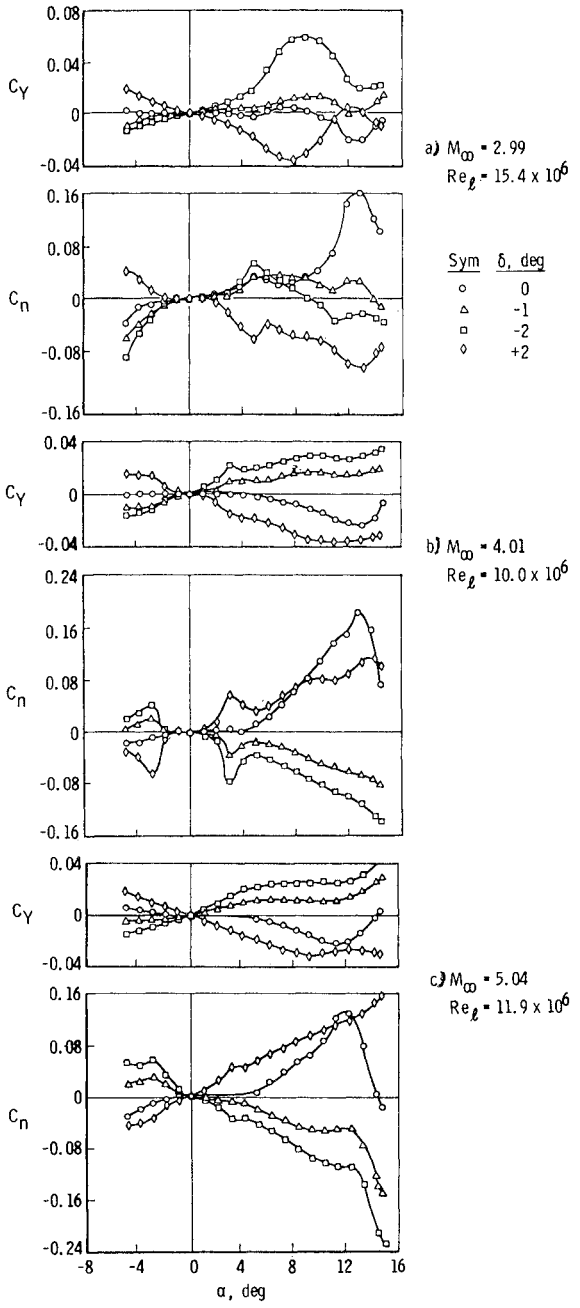

Fig. 11 Variations of C_Y and C_n with α for $\delta = 0°, -1°, -2°$, and $2°$; a) $M_\infty = 3$, b) $M_\infty = 4$, c) $M_\infty = 5$.

0° canted fin static data indicated larger forces from the body vortices.

From an examination of the various Magnus effects on this particular vehicle it appears that the body, windward fin, yaw couple, and possibly the body vortex system interaction with the fins would all contribute significantly to side loads. The body Magnus force and moment act in the same direction as the windward fin force and moment, and therefore the combined moment will possibly be greater than the yaw couple from the side fins. The body vortex system interaction with the fins may be a notable factor, particularly at the lower Mach numbers.

Examination of the Combined Magnus Effects

The variation of spin parameter $pd/2V_\infty$ with α is given in Fig. 10 for the various fin cant angles and Mach numbers. There was no notable change in spin rate between the Reynolds numbers at any one Mach number, and therefore, only one set of data at each Mach number is presented. This is as expected, since increasing the Reynolds number would increase both the rolling moment produced by the fin and also the roll damping. Throughout the report the data obtained with the model spinning will be identified by the fin cant angle, and the reader may refer back to Fig. 10 to obtain $pd/2V_\infty$. The spin rate was near constant over the α range tested for most of the configurations, and no analysis of any of the small variations was attempted since no attempt was made to monitor the bearing friction or to hold it constant.

In Fig. 11 the variations of C_y and C_n with α are presented for fin cant angles of 0°, −1°, −2°, and 2° at M_∞ = 3, 4, and 5. The data for $\delta = +2°$ and $-2°$ are very symmetric about the α axis at the lower α's. At the higher α's, where the zero spin data are affected by the asymmetric vortex pattern, the spin data in some cases are not symmetric for the two-different spin directions. This is especially apparent in the $M_\infty = 3$ yawing moment data (Fig. 11a).

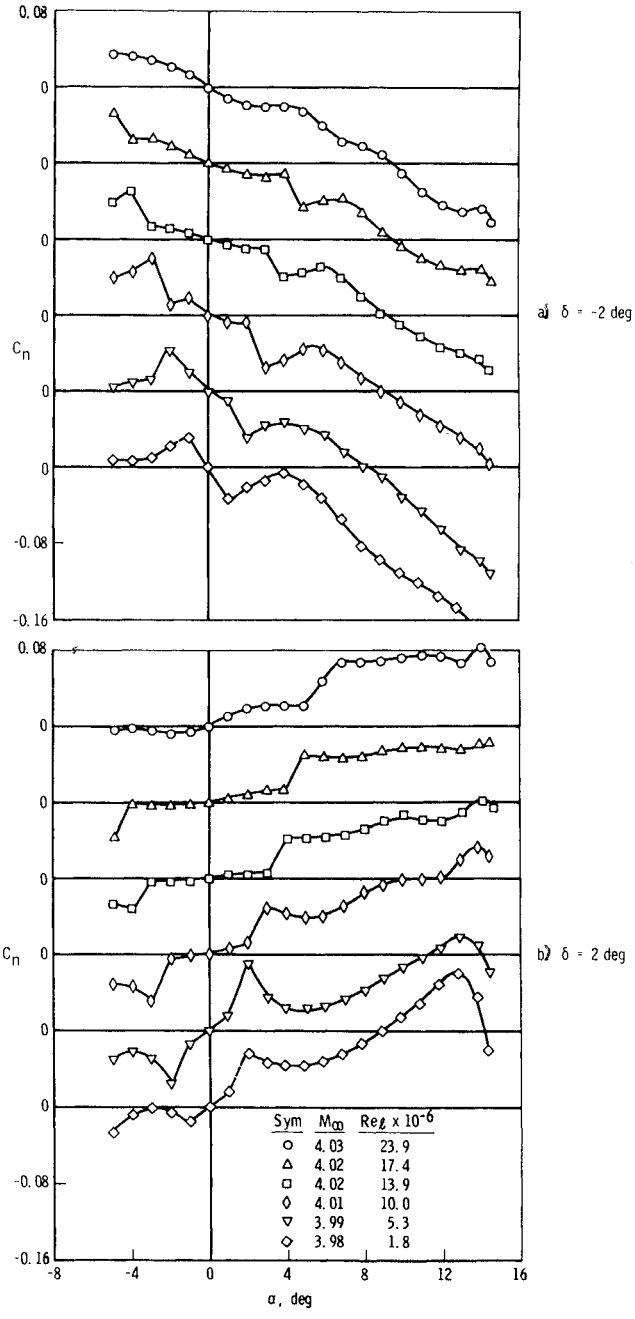

Fig. 12 Reynolds number effects at $M_\infty = 4$; a) $\delta = -2°$, b) $\delta = +2°$.

A second notable characteristic of these data is the sign change in the yawing moment between $M_\infty = 5$ and 3. The data show, for example, a positive C_n for $\delta = +2°$ at $M_\infty = 5$ (Fig. 11c) and a negative C_n for $\delta = +2°$ at $M_\infty = 3$ (Fig. 11a). The sign of C_y and C_n at $M_\infty = 4$ and 5 indicate that the effect of the windward fin and the body Magnus effect were predominant. Considering the previously presented body-alone Magnus data and the static data on the side loads at $M_\infty = 3$, and the fact that the effect of the body vortex system was most pronounced at $M_\infty = 3$, it appears that the change of sign of the yawing moment can be attributed mainly to the interaction of the body vortices on the fins.

Another interesting feature of the data is the nonlinearity exhibited in the yawing moment curve at $M_\infty = 4.01$, Re_l is 10×10^6 at the low α's ($\pm 3°$). The sharp slope reversal is well defined and symmetrical for positive and negative α's for both spin directions. This effect is also present, but not as pronounced in the $M_\infty = 2.99$, $Re_l = 15.4 \times 10^6$ and $M_\infty = 5.04$, $Re_l = 11.9 \times 10^6$ data. Since this phenomenon appeared to be a Reynolds number effect, the $-2°$ and $+2°$ fins were tested at $M_\infty = 4$ at Reynolds numbers ranging from $Re_l = 1.8 \times 10^6$ to $Re_l = 23.9 \times 10^6$. The data are presented in Fig. 12. The C_n data show clearly a step effect which occurs at $\alpha = 6°$ at $Re_l = 23.9 \times 10^6$ and dramatically moves down in α with decreasing Re_l. It is not known at this time what aerodynamic mechanism produces this effect.

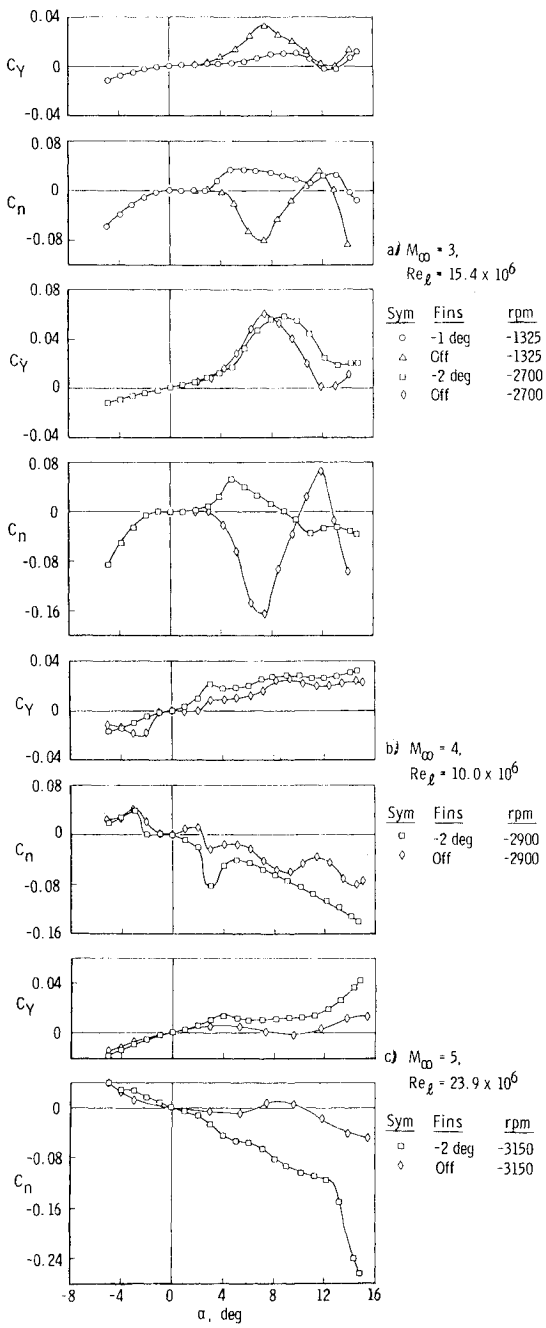

Fig. 13 Effects of fins on the C_Y and C_n variations with α; a) $M_\infty = 3$, $Re_l = 15.4 \times 10^6$; b) $M_\infty = 4$, $Re_l = 23.9 \times 10^6$; c) $M_\infty = 5$, $Re_l = 23.9 \times 10^6$.

The effects of the fins on the side force and yawing moment variations with α for the spinning model are shown in Fig. 13. The data for the no-fin model are presented at a spin rate equivalent to that for the fins-on configurations at $\delta = -1°$ and $-2°$, for $M_\infty = 3$, 4, and 5. The fin effects are different for the three Mach numbers. At $M_\infty = 5$, the body Magnus effects are small, and the fins contribute significant Magnus effects to the actual vehicle. The positive direction of C_Y indicates the dominance of the windward fin effect. At approximately $\alpha = 12°$ there is a rapid increase in the magnitude of C_Y and C_n which could be caused by either the windward fin moving more directly into the bow shock or a body vortex interaction with the leeward fin or a combination of these effects.

At $M_\infty = 3$ there are large differences between the fins-off and fins-on data. Again it appears that the body leeward vortex system greatly influences the results. Both the fins-off and fins-on data have large oscillations with α. These oscillations are attributed to vortices gradually building up and then being shed along the body. As a vortex is shed and a new one formed near the model base, the longitudinal pressure distribution on the sides of the model would be greatly altered causing reversals in the coefficients.

Concluding Remarks

A study of the Magnus effects at Mach numbers from 2 to 6 on a high-fineness-ratio ($l/d = 24.88$) sounding rocket indicate the following conclusions. 1) Side loads were measured on the nonspinning symmetrical model and are attributed to a steady asymmetric leeward vortex pattern. 2) The effects of the asymmetric vortex pattern was more pronounced at the lower Mach numbers. 3) The body Magnus force decreased with increasing Mach number. 4) The body Magnus force increased with Reynolds number. 5) There were no measurable side loads from the fin blanket effect. 6) The canted windward fin produced appreciable Magnus effects. 7) The fin yaw couple effect was of significant magnitude. 8) The data indicated that the Magnus effects produced on the spinning model by the interaction of the body vortices with the fins were appreciable at the lower Mach numbers. 9) The data indicate that the vortex interaction caused the Magnus moment on the fins-on configuration to be in the opposite direction for $M_\infty = 3$ than for $M_\infty = 4$ and 5. 10) The data show a significant effect of Reynolds number.

References

[1] Falanga, R. A., "Supersonic Investigation of a Spinning and Nonspinning Model of a Cajun (or Apache) Rocket Vehicle with Roll-Control Tabs," TN-D-2576, Jan. 1965, NASA.

[2] Uselton, J. C., "Investigation of the Magnus Effects and the Effects of Unsymmetrical Leeward Vortex Patterns on a High Fineness Ratio Model at Mach Numbers 3 and 5," M.S. thesis, Aug. 1966, Univ. of Tennessee, Knoxville, Tenn.

[3] Curry, W. H. and Reed, J. F., "Measurement of Magnus Effects on a Sounding Rocket Model in a Supersonic Wind Tunnel," AIAA Paper 66-754, Los Angeles, Calif., 1966.

[4] Curry, W. H., Reed, J. F., and Uselton, J. C., "Some Comments on the Aerodynamic Characteristics of the Tomahawk Sounding Rocket," *AIAA Sounding Rocket Vehicle Technology Specialist Conference*, AIAA, New York, 1967.

[5] Allen, H. J. and Perkins, E. W., "Characteristics of Flow over Inclined Bodies of Revolution," RM A50L07, March 1951, NACA.

[6] Gowne, F. E. and Perkins, E. W., "A Study of the Effects of Body Shape on the Vortex Wakes of Inclined Bodies at a Mach Number of 2," RM A53I17, Dec. 1953, NACA.

[7] Gowen, F. E., "Buffeting of a Vertical Tail on an Inclined Body at Supersonic Mach Numbers," RM A53A09, March 1953, NACA.

[8] Thompson, K. D. and Morrison, D. F., "On the Asymmetric Shedding of Vortices from Slender Cylindrical Bodies at Large Angles of Yaw," TN HSA 106, May 1965, Australian Defense Scientific Service, Weapons Research Establishment, Salisbury, South Australia.

[9] Cooper, M., Gapcynski, J. P., and Hasel, L. E., "A Pressure-Distribution Investigation of a Fineness-Ratio-12.2 Parabolic Body of Revolution (NACA RM-10) at M = 1.59 and Angles of Attack up to 36°," RM L52G14a, Oct. 1952, NACA.

[10] Letko, W., "A Low-Speed Experimental Study of the Directional Characteristics of a Sharp-Nosed Fuselage Through a Large Angle-of-Attack Range at Zero Angle of Sideslip," TN 2911, March 1953, NACA.

[11] Platou, A. S., "Magnus Characteristics of Finned and Non-Finned Projectiles," *AIAA Journal*, Vol. 3, No. 1, Jan. 1965, pp. 83–90.

[12] Platou, A. S., "The Magnus Force on a Finned Body," Rept. 1193, March 1963, Ballistics Research Lab., Aberdeen Proving Ground, Md.

[13] Benton, E. R., "Supersonic Magnus Effect on a Finned Missile," *AIAA Journal*, Vol. 2, No. 1, Jan. 1964, pp. 153–155.

[14] Kelly, H. R. and Thacker, G. R., "The Effect of High Spin on the Magnus Force on a Cylinder at Small Angles of Attack," Navard Rept. 5036, Feb. 1956, Naval Ordnance Test Station, China Lake, Calif.